Effect of the Air−Water Interface on the Stability of β-Lactoglobulin

ARTICLE *in* THE JOURNAL OF PHYSICAL CHEMISTRY B · JANUARY 2008

Impact Factor: 3.3 · DOI: 10.1021/jp074777r · Source: PubMed

4 AUTHORS, INCLUDING:

Stephen Andrew Holt

Australian Nuclear Science and Technology …

87 PUBLICATIONS **972** CITATIONS

Effect of the Air−Water Interface on the Stability of β-Lactoglobulin

Adam W. Perriman,[†] Mark J. Henderson,[†] Stephen A. Holt,[‡] and John W. White*[,†]

Research School of Chemistry, Australian National University, Canberra ACT 0200, Australia, and ISIS, CCLRC Rutherford Appleton Laboratory, Chilton, Didcot, Oxon UKO X110 QX

Received: June 20, 2007; In Final Form: August 24, 2007

We report the X-ray and neutron reflectometry measurements of the structural changes caused by chemical denaturation of a surface excess of the bovine milk protein, β-lactoglobulin. The thickness of the diffuse protein surface layer was used as an order parameter as there was no corresponding increase in the surface excess as a function of guanidinium chloride (G.HCl) concentration. A thermodynamic analysis performed gave the interfacial free energy of unfolding in the absence of a denaturant (ΔG^0). This energy, lower than the free energy of unfolding bulk solution, shows that the air−water interface has a destabilizing effect on protein structure up to 50 kJ mol^{-1}.

1. Introduction

Protein adsorption at air−liquid interfaces is of fundamental interest in understanding physiological processes, such as protein delivery in secondary hemostasis,[1] and industrial significance through foam stability in food processing.[2] With increasing interest in de novo approaches to designing surface active peptides,[3] and microarray technologies,[4] understanding the effect of adsorption on protein structure and stability is essential. Exposing proteins to increasing concentrations of chemical denaturants is performed routinely to provide information on the stability of proteins in solution.[5] However, less research has been conducted on proteins adsorbed at the air−water interface with a view to quantifying the effect of this interface on protein stability. In this study, we report the changes in structure of β-lactoglobulin adsorbed at the air−solution interface as a function of guanidinium chloride (G.HCl) and urea concentration and compare the behavior with that reported for the same protein denatured in solution.

β-Lactoglobulin is a small soluble globular protein (approximately 18×10^3 g mol^{-1}) containing 162 amino acids per monomer. It exists as a dimer under physiological conditions,[6] and its isoelectric point (p*I*) is at pH 5.3.[7] The overall topology of the protein was first described using X-ray crystallography in 1986 at a resolution of 2.8 Å.[8] Since that time, a number of high-resolution crystal structures have been published highlighting the structural features that have led to the classification of β-lactoglobulin as a lipocalin.[9,10] All members of the lipocalins[9] have β-barrels composed of eight parallel β-strands, where each successive β-strand is adjacent to the preceding one. Each monomer also contains two disulfide bonds formed by the reaction of the thiol groups of Cys160 and Cys66, Cys119 and Cys106, as well as the one free thiol of Cys121.[10] The presence of the two disulfide bonds allows β-lactoglobulin to retain a globular structure, showing remarkable stability and a resistance to acid-denaturation,[11] maintaining its native structure even at pH 2.

The dimensions of the β-lactoglobulin monomer and dimer are 40 Å × 44 Å × 37 Å[12] and 77 Å × 44 Å × 42 Å,[13] respectively. Neutron reflectometry measurements of β-lactoglobulin adsorbed both at the air−water[14] and the hydrophobic solid−liquid[15] interface have shown protein surface layer thicknesses close to that of the shortest axis (36 Å) of the monomer, suggesting little or no change to the globular structure upon adsorption. Supporting this view, infrared reflection absorption spectroscopy (IRRAS) studies have shown limited changes to the secondary structure of β-lactoglobulin on adsorption at the air−water interface.[16,17]

The structure of proteins containing a high proportion of nonpolar or hydrophobic residues have been shown to be less stable at the air−water interface than those proteins containing less.[18,19] This effect could be viewed as the inverse of the hydrophobic effect. The hydrophobic effect is viewed as a primary driving force for protein folding through entropic gains made by burying hydrophobic residues in the interior of proteins.[20] However, if the surface of a protein is exposed to the air upon adsorption, an alternative lowest energy structure may be prevalent where some hydrophobic residues are no longer buried but can present to the air.

For adsorbed protein molecules, the secondary, tertiary, and quaternary structures are subject to asymmetric interfacial interactions on the molecular cohesive forces. The degree of surface denaturation depends on the structural characteristics of the protein molecule. For example, Min et al. showed that the presence of covalent disulfide bonds reduced the level of structural distortion and the surface activity of globular protein molecules adsorbed at the air−water interface.[21]

A complete understanding of how chemical denaturants unfold proteins is yet to emerge. Within the field of denaturation methodology, two theories predominate. The first is that the phenomenon results from changes in solvent properties at high concentrations of chemical denaturants leading to a change in the structure of water.[22−25] The second theory suggests that there is a more specific denaturant−protein interaction, by which the denaturants promote protein unfolding through positive interactions with buried residues exposed upon unfolding.[20,26]

Differences in denaturation mechanisms may be illustrated by comparing the effect of G.HCl and urea. D'Alfonso et al. suggest that an electrostatic contribution dominates when G.HCl

* To whom correspondence should be addressed. E-mail: jww@rsc.anu.edu.au. Phone: +61 (2) 6125-3578. Fax: +61 (2) 6125-4903.
[†] Australian National University.
[‡] CCLRC Rutherford Appleton Laboratory.

10.1021/jp074777r CCC: $37.00
Published on Web 11/10/2007

is used to denature β-lactoglobulin.[27] Dempsey and co-workers investigated the difference in specificity between these two denaturants by conducting unfolding experiments on both an alanine-based helical peptide (which is free of side chain electrostatic contributions) and a tryptophan zipper peptide.[28] The authors were able to show that G.HCl is only slightly more effective than urea at attenuating H bonds but much more effective against indole−indole interactions (representing hydrophobic interactions).

Molecular dynamics simulations applied to recent neutron diffraction data have shown significant ion pairing for the charged guanidinium ions, indicating preference for a stacked structure at 3 mol dm^{-3} and 25 °C.[29] In this arrangement, the N−H groups form well-ordered hydrogen bonds in the molecular plane, but the planar faces themselves are hydrophobic. From this the authors proposed a mechanism by which the guanidinium ion can unfold a protein through association with the hydrophobic side chains and through formation of H bonds with water and polar side chains.

In this work, we demonstrate the ability to track the changes in the equilibrium surface-structure of β-lactoglobulin with increasing concentrations of the two denaturants, G.HCl and urea, with reflectometry using neutrons and X-rays. The data from these experiments are subsequently analyzed using the thermodynamic protocol described below (see the Experimental Procedures, section 2.2. Methodology), providing quantitative information on the effect of the air−water interface on the stability of the protein.

2. Experimental Procedures

2.1. Materials. Bovine β-lactoglobulin (L0130) was used as received from Sigma Aldrich. The lyophilized β-lactoglobulin was from bovine milk containing genetic variants A and B of purity greater than 95% (SDS-PAGE). The concentration of β-lactoglobulin solutions was 10 mg mL^{-1} containing 100 ppm sodium azide to inhibit bacterial growth. For neutron reflectometry experiments, protein solutions were made using air-contrast-matched-water (ACMW) deoxygenated with high purity nitrogen. The protein was dissolved in this deoxygenated water by gently swirling in a conical flask before being transferred quantitatively to a volumetric flask. ACMW is a heavy−light water mixture so constituted that its coherent neutron scattering length density (Nb_n) is zero; thus, it is "invisible" to neutrons and therefore is null reflecting. The addition of G.HCl, however, contributed appreciably to the scattering length density of the solution for all the denaturant concentrations studied. Only those solutions containing no denaturant were completely contrast matched. All solutions were produced using a phosphate buffer (5×10^{-2} mol dm^{-3} $H_2PO_4^-/HPO_4^{2-}$), were kept at 4 °C, and used within 1 day of preparation. Stock G.HCl or urea solutions and stock protein solutions were combined in a conical flask and mixed thoroughly for 2 min immediately before pouring into a PTFE sample cell. Each cell was temperature controlled and was sealed hermetically after exposure to a nitrogen atmosphere at 25 °C. Measurements were recorded immediately as well as after a minimum of 50 min to allow equilibrium between the subphase and the surface to be established.

X-ray reflectometry experiments were performed on β-lactoglobulin solutions in Milli-Q quality water at 16 guanidinium chloride concentrations (0 to 3.5 mol dm^{-3}) and 8 urea concentrations (0−6 mol dm^{-3}). Disulfide bond reduction experiments were performed using both 0.02 and 0.10 mol dm^{-3} dithiothreitol (DTT) containing 0.002 mol dm^{-3} ethylendiaminetetraacedic acid (EDTA) in buffer only and in a buffered 6 mol dm^{-3} urea solution.

2.2. Reflectometry and Data Analysis. The neutron reflectivity profiles were measured using the SURF and the CRISP reflectometers at the ISIS spallation neutron source at the Rutherford Appleton Laboratory, Oxfordshire U.K.[30] Alignment of both instruments was confirmed by measuring the reflectivity of pure D_2O and comparing the model parameters with known values. All subsequent experiments were scaled using the reflectivity of D_2O. A super-mirror was employed for all experiments to allow reflectivity to be detected over an increased Q_z range. The incident beam angles were 0.35°, 0.50°, 0.80°, and 1.50° corresponding to Q_z ranges of 0.01−0.25 $Å^{-1}$. However, since solutions were made using ACMW, the minimum measurable reflectivity was restricted by the incoherent background scattering from the sample. As a consequence, only data up to 0.125 $Å^{-1}$ were modeled.

X-ray reflectometry measurements were recorded using the angle dispersive instrument[31] at the rotating anode source of the Research School of Chemistry, ANU. The Cu Kα radiation was selected using a graphite (002) monochromator. Alignment of the instrument was achieved by measuring the reflectivity of Milli-Q quality water and comparing the model parameters with known values.[32] Measurements were made at angles of incidence in the range of 0.00−0.35 $Å^{-1}$, and all data was scaled using the critical edge of a given sample.

The reflectivity measurements were modeled using CXMULF,[31] a program incorporating the optical transfer matrix method[33] of classical optics. Model parameters used in this program are τ, the film thickness (Å), Nb_x, the X-ray scattering length density ($Å^{-2}$), Nb_n, the neutron scattering length density ($Å^{-2}$), and σ, the Gaussian interfacial roughness (Å) of a series of homogeneous slabs. X-ray and neutron data sets were fitted individually and finally co-refined.

Co-refining X-ray and neutron datasets increases the probability of finding a unique solution. Although the data both from both techniques are modeled using parameters that are essentially analogous (τ, σ, Nb_x, and Nb_n), differences in the Q_z resolution between the techniques results in the need for further adjustment to the model. Specifically, when refined independently, the higher resolution X-ray dataset may require a two-layer model, whereas a single layer model is sufficient for the lower resolution neutron dataset of the same sample. In this case, the single neutron layer thickness was modeled as the sum of the two X-ray layers.

2.3. Methodology. For protein solutions containing G.HCl, reflectometry experiments using both X-rays and neutrons allow evaluation of the surface excess directly, without knowledge of the protein density. An estimate of the sum of the neutron scattering lengths of the subphase ($\sum b_{sub}$, Å) can be obtained using eq 1

$$\sum b_{sub} = \frac{Nb_{n\_sub}\langle M_W \rangle}{\rho_{sub} N_A} \tag{1}$$

where Nb_{n_sub} is the measured subphase scattering length density, ρ_{sub} is the physical density of the subphase, and $\langle M_W \rangle$ is the molecular weight average of all components in the subphase. The average volume occupied by a protein can also be estimated using eq 2

$$V_{prot} = \frac{r_0\left(\sum Z_{prot} - n\left\langle \sum Z_{sub} \right\rangle\right)}{Nb_x} \tag{2}$$

where $\langle\sum Z_{sub}\rangle$ is the average of the sum of electrons in the subphase and n is given by eq 3

$$n = \frac{r_0 N b_n \sum Z_{prot} - N b_x \sum b_{prot}}{N b_x \sum b_{sub} - r_0 N b_n \langle \sum Z_{sub} \rangle} \quad (3)$$

Now that the average volume has been evaluated using eq 2, the surface excess can be obtained using eq 4

$$\Gamma = \frac{10^{20} M_W \tau}{N_A V_{prot}} \quad (4)$$

In order to use eqs 1−4, the physical densities of the solutions must be known accurately, so that the subphase (D_2O, H_2O, and G.HCl) can be treated as a continuous liquid phase of known scattering length density. In the present study, these values were taken from the literature.[34] Ideal mixing of guanidinium chloride and water is only assumed when considering potential partitioning of the guanidinium chloride between the subphase and surface layer through interactions with the protein molecules at the air−water interface. Using XRD, Mande and Sobhia were able to locate 2 bound guanidinium ions per lysozyme molecule which would have little effect on the composition of the continuous phase at the air−water interface.[35] Courtenay et al., however, showed preferential protein surface partitioning by guanidinium in a study using bovine serium albumin (BSA).[36] From Courtenay's osmolality data and the osmotic coefficients provided in Macaskill et al.,[37] the number of guanidinium ions associated with a single BSA molecule is approximately 10 at 1.0 mol dm^{-3}.

To estimate the average number of guanidinium ions associated with each β-lg monomer from the BSA data, the solvent accessible surface areas (SASA) of the hydrophobic and hydrophilic regions of each protein were calculated and compared using the POPS[38] (parameter optimized surfaces) algorithm. If the SASA (and hydropathy) is used to approximate the extent of denaturant association, the number of guanidinium ions associated with each β-lg molecule would expect to range from 1 at 0.2 mol dm^{-3} to 10 at 2.5 mol dm^{-3} (after extrapolating Courtenay's data out to 2.5 mol dm^{-3} which shows 33 guanidinium ions per BSA molecule). At a G.HCl concentration of 2.5 mol dm^{-3}, this would lead to an overestimation of the protein surface excess by about 5%, where the uncertainties in this value are typically 10%.

Differences in the protein volume between the bulk solution and the air−water interface may arise from two mechanisms: (1) a change in the tertiary structure of the protein resulting from exposure of the protein to the surface environment and (2) the effect of hydration or lack thereof for those groups exposed to the air. To varying extents, both of these phenomena have been reported, e.g., structural distortion of myoglobin at the air−water interface,[39] and the exposure of adsorbed hen egg white lysozyme to air.[40]

For single-contrast X-ray reflectometry experiments, the total volume of the protein can be estimated from literature amino acid residue volumes.[41] Subsequently, the X-ray scattering length density of the pure protein, Nb_{x_prot}, may be calculated by simply adding up the number of electrons in a single protein unit

$$Nb_{x\_prot} = \frac{\sum Z_{prot} r_0 N_A \rho_{prot}}{M_W} \quad (5)$$

where $\sum Z_{prot}$ is the number of electrons in a protein molecule, r_0 is the classical electron radius (2.8×10^{-5} Å), and ρ_{prot} is the physical density of pure protein. Once the theoretical scattering length density of the pure protein is evaluated, eq 6 can then be used to evaluate of the volume fraction of protein normal to the surface plane (ϕ_{prot})[14]

$$\phi_{prot} = \frac{Nb_{x\_sub} - Nb_x}{Nb_{x\_sub} - Nb_{x\_prot}} \quad (6)$$

where Nb_{x_sub} and Nb_x are the X-ray scattering length densities of the subphase and the layer respectively. The surface excess (Γ) can also now be evaluated using eq 7

$$\Gamma = \tau \phi \rho_{prot} \quad (7)$$

2.4. Chemical Denaturation Thermodynamics. Since Greene and Pace demonstrated that the plots of the free energy of unfolding were linear in denaturant concentration for both urea and guanidinium chloride,[42] the linear extrapolation model has become the most applied procedure for obtaining ΔG^0 from denaturant-induced unfolding transitions. The linear extrapolation model is purely phenomenological and ΔG^0 is obtained by extrapolation of $\Delta G'$ values observed in the transition zone back to zero denaturant concentration.

$$\Delta G' = \Delta G^0 + m[D] \quad (8)$$

where m is the slope describing the dependence of ΔG on the molar denaturant concentration, [D]. The population of the protein molecules over the two states has been described in this work by use of the film thickness, τ, for the following equilibrium:

$$N \overset{K}{\rightleftharpoons} U \quad (9)$$

where N and U represent the native and unfolded states respectively. The observed protein film thickness is a function of the concentration of the chemical denaturant [D]. At a given τ is approximately

$$\tau = f_N \tau_N + f_U \tau_U \quad (10)$$

where τ_N is the protein layer thickness for the native state and f_N denotes the fraction of protein in the nth state where

$$f_N + f_U = 1 \quad (11)$$

Combining eq 10 with eq 11 yields

$$\tau = f_N + \tau_U - \tau_U f_N \quad (12)$$

The equilibrium constant K for eq 9 can be defined as

$$K = \frac{[U]}{[N]} \quad (13)$$

where [N] and [U] represent the concentration of protein in the native and unfolded states respectively. Expressing the equilibrium constants in terms of the parameters defined in eq 11 gives

$$K = \frac{1 - f_N}{f_N} \quad (14)$$

Thus, the relative fraction of protein in a given state can be expressed as a function of the equilibrium constants by

$$f_U = \frac{K}{K+1} \tag{15}$$

$$f_N = \frac{1}{K+1} \tag{16}$$

Substituting eqs 15 and 16 into eq 12 gives

$$\tau = \tau_U + \frac{\tau_N - \tau_U}{K+1} \tag{17}$$

The Gibbs free energy change defined in terms of the equilibrium constant K is

$$\Delta G' = -RT \ln K \tag{18}$$

Thus, the equilibrium constant for the first transition is defined using the linear extrapolation method by combining eq 8 with eq 18

$$K = \exp\left(\frac{-\Delta G^0 + m[D]}{RT}\right) \tag{19}$$

Finally, by using eqs 19 and 17, it is possible to express the thickness of the protein layer as a function of denaturant concentration

$$\tau = \tau_U + \frac{\tau_N - \tau_U}{1 + e\dfrac{RT}{\Delta G^0 + m[D]}} \tag{20}$$

Thus, the protein layer thickness can be plotted as a function of denaturant concentration, and by applying nonlinear regression using eq 20, it is possible to evaluate m as well as the Gibbs free energy change of unfolding for each transition.

The approach used above can also be used to describe a three-state unfolding mechanism

$$N \overset{K_1}{\rightleftharpoons} I \overset{K_2}{\rightleftharpoons} U \tag{21}$$

where I represents the intermediate state, and the equilibrium constants K_1 and K_2 are given by

$$K_1 = e^{(-\Delta G_1{}^0 + m_1[D])/RT} \tag{22}$$

and

$$K_2 = e^{(-\Delta G_2{}^0 + m_2[D])/RT} \tag{23}$$

The equilibrium constants are now related to the observed film thickness (τ) by

$$\tau = \tau_N + \frac{K_1(\tau_I - \tau_N + K_2\tau_U - K_2\tau_N)}{1 + K_1K_2 + K_1} \tag{24}$$

3. Results

3.1. Time Dependence of the Interfacial Structure of Unreduced β-Lactoglobulin at 25 °C. The structural changes of the 10 mg mL^{-1} β-lactoglobulin solution without a denaturant present (the control experiment) were negligible. After equilibration for 2 h, no significant change in the X-ray reflectivity pattern was observed for 24 h. Also, no perceptible change of the reflectivity curves obtained from solutions containing a chemical denaturant was detected over the same time period even at the highest concentrations studied. These results indicate that both the protein and denaturant were necessary to cause changes in the reflectivity profiles.

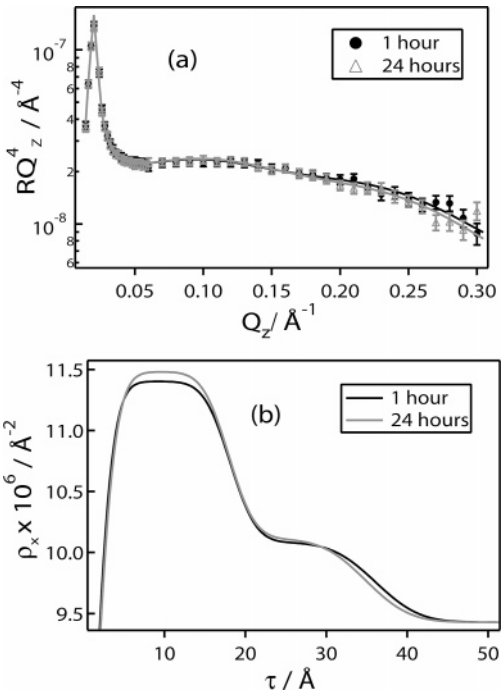

Figure 1. (a) X-ray RQ_z^4 vs Q_z profiles and fits (line) and (b) real-space X-ray scattering length density profiles obtained at the air−water interface from a 10 mg mL^{-1} β-lactoglobulin solution containing a standard phosphate buffer. Measurements were recorded after 1 h (black line) and after 24 h (gray line).

Figure 1a shows the RQ_z^4 vs Q_z X-ray reflectivies obtained from 10 mg mL^{-1} β-lactoglobulin solutions as at 1 and 24 h. A two layer model was used to extract the layer thickness and the scattering length densities. The resulting real space scattering length density profile is presented in Figure 1b. The overlaid profiles do not show any significant differences. At the air−water interface, the scattering length density rises from zero as defined for air. Below the interface, a 36 Å region extends into the subphase, consisting of a dense upper layer of 18 Å, a diffuse 18 Å layer, and at large distances an X-ray scattering length density (9.43×10^{-6} Å^{-2}) equal to that of the subphase.

3.2. Structure Dependence on Guanidinium Chloride Concentration. In order to investigate the effect of [G.HCl] on the surface structure of β-lactoglobulin, experiments were performed using both neutrons and X-rays over a denaturant concentration range of 0.0−3.5 mol dm^{-3}. The differences in the reflectivity curves across this range are evident: those obtained from solutions containing a low concentration of G.HCl are more reflective at high Q_Z (Figures 2 and 3). Neutron reflectivity was not possible from a solution containing 3.5 mol dm^{-3} solutions as the reflectivity was low, because of surface roughening effects. The data were refined using two layer and three layer models, depending upon the [G.HCl]: at high [G.HCl], three layer models were necessary. The fitting parameters are summarized in Table 1.

Figure 3b provides a comparison between the X-ray scattering length density profiles resulting from the control protein solution containing no denaturant and the highest G.HCl concentration, 3.5 mol dm^{-3}, studied. The data obtained from the highest denaturant concentration reveal an uppermost layer with a scattering length density lower than water. This layer, which represents the upper 14 Å of the protein molecule, is believed

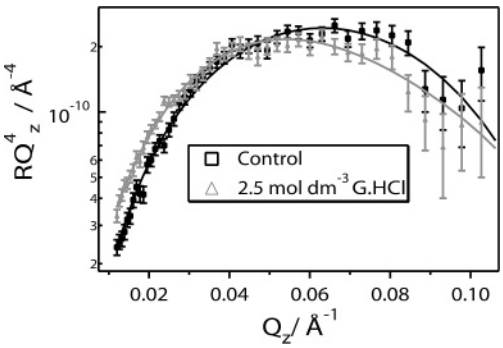

Figure 2. RQ_z^4 vs Q_z neutron reflectivities and fits (solid line) obtained at the air−water interface from a 10 mg mL^{-1} β-lactoglobulin solutions containing 0.0 (black squares) and 2.5 mol dm^{-3} (red triangle) G.HCl.

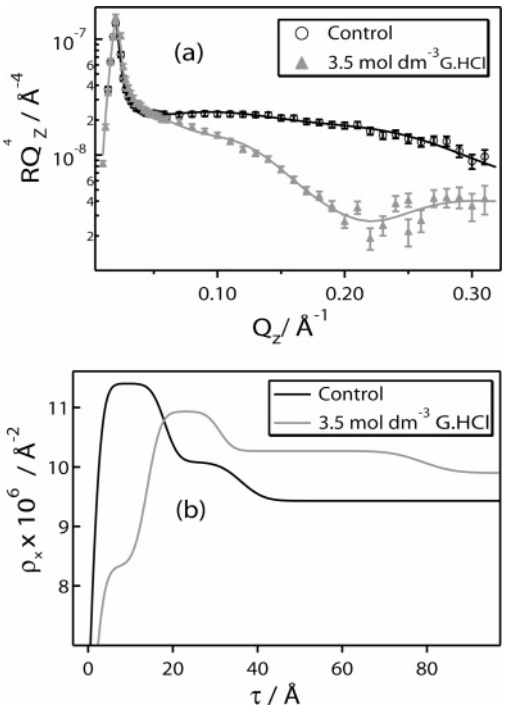

Figure 3. (a) RQ_z^4 vs Q_z X-ray reflectivities and fits (solid line) and (b) real-space X-ray scattering length density profiles obtained at the air−water interface from 10 mg mL^{-1}β-lactoglobulin solutions containing 0.0 (black) and 3.5 mol dm^{-3} (gray) G.HCl.

to be dehydrated as a result of its exposure to the air. Protein dehydration has previously been reported for lysozyme at the air−water interface where the upper 10 Å was exposed.[40] The formation of a diffuse scattering length "tail" is apparent extending down to a depth of approximately 90 Å.

Figure 4 shows the variation of the layer thicknesses with G.HCl concentration for two layer models (≤1.0 mol dm^{-3} G.HCl) and three layer models (above this concentration). As the denaturant concentration is increased, the solutions containing moderate concentrations of denaturant, 0 to 2.0 mol dm^{-3} display little change in the thickness of the layer closest to the air, maintaining a thickness near to that of the control solution. At [G.HCl] = 2.5 mol dm^{-3}, a sudden increase in the upper layer thickness is observed, followed by a reduction at 3.5 mol dm^{-3} where surface penetration is occurring. The thickness of the second layer increased when the denaturant was introduced, expanding to about 35 Å at [G.HCl] = 2.5 mol dm^{-3}. Denaturation, as shown by the growth of a low density "tail" deep into the subphase, is apparent at [G.HCl] = 2.0 mol dm^{-3} and pronounced at [G.HCl] = 2.5 and 3.5 mol dm^{-3}.

3.3. Structure Dependence on Urea Concentration. In order to investigate denaturant-specific effects including charge considerations, X-ray reflectivity measurements were recorded as a function of urea concentration. The surface structure was monitored in the denaturant range of 0−6 mol dm^{-3} urea. A two layer model was used for urea concentrations from 0 to 2.0 mol dm^{-3}, and a third layer was required for concentration of 2.5 mol dm^{-3} and above. The fitting parameters are summarized in Table 2. In Figure 5a the RQ_z^4 vs Q_z reflectivities for the control protein solution and the protein solution containing 6.0 mol dm^{-3} urea have been superimposed. In a similar manner to that observed for β-lactoglobulin in the presence of high levels of G.HCl, the reflectivity was lower at Q_Z values >0.05 Å^{-1} for the solution containing urea.

Figure 5b displays the X-ray scattering length density profiles resulting from the data fitting in Figure 5a. At [urea] = 6.0 mol dm^{-3}, three layers differing in density can be distinguished. A 20 Å dense upper layer is followed by a 20 Å layer of moderate density, with a diffuse 40 Å "tail" blending into the subphase. The formation of the low scattering length density "tail" was also observed for β-lactoglobulin denatured by [G.HCl] = 3.5 mol dm^{-3}, although for urea exposure and subsequent dehydration of the surface layer did not occur.

As the urea concentration was increased, an increase in the solution scattering length density occurred. At 6.0 mol dm^{-3}, the scattering length density of the subphase was 10×10^{-6} Å^{-2}, an increase of about 6%. This increase results in a positive offset in the X-ray scattering length density profile. This has two further effects: (i) a reduction in contrast between the solvent and the protein and (ii) an increase in the X-ray scattering length density of all solvent-containing layers. Though an increase in the X-ray scattering length density of the second layer is significant, there is little change in the layer adjacent to air.

Figure 6 shows the variation of the layer thickness parameters with urea concentration. The thicknesses of both the upper layer adjacent to air and the middle layer remain relatively constant over the entire concentration range. This is in contrast to the G.HCl experiments where there was an immediate dilation of the middle layer. Formation of the lower diffuse layer is evident at a urea concentration of 2.5 mol dm^{-3} with a thickness of approximately 30 Å. As the urea concentration was raised further, this layer thickness reaches a final value of over 40 Å at 6.0 mol dm^{-3}.

3.4. Effect of Disulfide Bonds on the Equilibrium Structure: Reduced β-Lactoglobulin. β-Lactoglobulin contains two disulfide bonds per monomer which contribute to the stabilization of the globular structure. To examine the response of the structure of β-lactoglobulin at the air−water interface to removal of these bonds, solutions of the protein containing dithiothreitol (DTT) were prepared. Two concentrations of DTT at 20×10^{-3} and 100×10^{-3} mol dm^{-3} were used.

At 20 mM, DTT appears to have only a minor effect on the surface structure of β-lactoglobulin at the air−water interface. There is a slight reduction in the thickness of the upper layer from 18 Å for native conditions to 16.5 Å under reducing conditions (data not shown). This variation, however, is near the limit of the resolution of the technique.

At a DTT concentration of 100 mM, changes in the reflectivity of adsorbed β-lactoglobulin were observed [Figure 7a]. An overall increase in the X-ray scattering length density of the surface layers and an 8 Å increase in the thickness of the lower layer, however, suggest changes in the tertiary structure

TABLE 1: Co-refined Neutron and X-ray Fitting Parameters Obtained from Modeling Data from 10 mg mL^{-1} Solutions of β-Lactoglobulin Containing Different Concentrations of Guanidinium Chloride

[G.HCl] /mol dm^{-3}	layer	τ /Å	$\sigma_{air-film}$ /Å	Nb_x /10^{-6} Å^{-2}	Nb_N /10^{-6} Å^{-2}	Γ^a /mg m^{-2}	Γ^b /mg m^{-2}
0.00	1	18.2 (0.7)	2.8 (0.5)	11.03 (0.05)	0.75 (0.01)	2.1 (0.1)	2.4(0.1)
	2	18.0 (0.9)		10.01 (0.06)	0.75 (0.01)		
0.02	1	18.5 (0.7)	2.8 (0.5)	11.03 (0.06)	0.75 (0.01)	2.1 (0.1)	2.4(0.1)
	2	17.2 (0.8)		10.01 (0.06)	0.75 (0.01)		
0.20	1	21.0 (1)	2.6 (0.5)	10.96 (0.05)	0.70 (0.01)	2.2 (0.1)	2.5 (0.1)
	2	26.5 (1)		10.18 (0.05)	0.70 (0.01)		
1.00	1	19.7 (1)	3.0 (0.5)	11.06 (0.06)	0.72 (0.01)	2.2 (0.1)	2.7 (0.1)
	2	32.1 (1)		10.24 (0.05)	0.72 (0.01)		
2.00	1	16.5 (1)	3.2 (0.5)	11.19 (0.1)	0.72 (0.01)	1.8 (0.2)	3.0 (0.2)
	2	33.4 (2)		10.31 (0.05)	0.72 (0.01)		
	3	28.1 (2)		9.99 (0.06)	0.35 (0.01)		
2.50	1	27.1 (1)	4.0 (0.5)	10.81 (0.04)	0.76 (0.01)	2.2 (0.2)	2.7 (0.2)
	2	21.1 (1)		10.30 (0.04)	0.76 (0.01)		
	3	30.6 (2)		10.03 (0.05)	0.31 (0.01)		
3.50	1	14.1 (0.5)	3.2 (0.9)	8.33 (0.04)			
	2	17.1 (1)		10.93 (0.05)			
	3	47.8 (3)		10.27 (0.05)			

[a] Evaluated using X-rays and neutrons. [b] Evaluated using X-rays only.

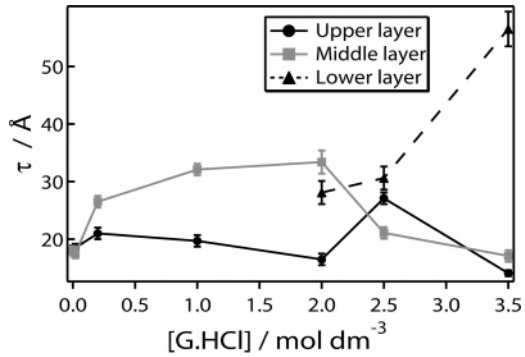

Figure 4. Variation of individual layer thicknesses with guanidinium chloride concentration. The upper layer (black circles with solid line) is adjacent to the air, and lower layer (gray triangles with broken line) is adjacent to the solution.

TABLE 2: X-ray Reflectometry Fitting Parameters from 10 mg mL^{-1} Solutions of β-Lactoglobulin Containing Different Concentrations of Urea

urea / mol dm^{-3}	layer	τ/ Å	$\sigma_{air-film}$ / Å	Nb_x / 10^{-6} Å^{-2}	Γ/ mg m^{-2}
0.00	1	18.2 (0.7)	2.7 (0.4)	11.03 (0.05)	2.4 (0.1)
	2	18.0 (1)		10.01 (0.06)	
1.50	1	18.5 (0.7)	2.7 (0.5)	11.36 (0.06)	2.2 (0.1)
	2	17.4 (1)		10.07 (0.07)	
2.0	1	20.8 (0.6)	2.6 (0.4)	11.19 (0.04)	2.1 (0.1)
	2	20.4 (1)		10.02 (0.05)	
2.5	1	21.5 (0.6)	2.5(0.3)	11.09 (0.04)	2.4 (0.1)
	2	17.9 (1)		10.20 (0.04)	
	3	30.0 (2)		9.86 (0.04)	
3.0	1	17.0 (0.6)	2.9 (0.5)	11.53 (0.06)	2.6 (0.2)
	2	17.7 (1)		10.43 (0.04)	
	3	45.6 (3)		9.90 (0.03)	
4.0	1	18.8 (0.7)	2.4 (0.5)	11.25 (0.05)	2.1 (0.1)
	2	21.2 (1)		10.25 (0.04)	
	3	33.7 (2)		9.91 (0.03)	
5.0	1	19.0 (0.5)	2.5 (0.3)	11.32 (0.04)	2.4 (0.1)
	2	18.4 (0.9)		10.38 (0.03)	
	3	41.1 (3)		10.01 (0.02)	
6.0	1	20.1 (0.5)	3.2 (0.3)	11.33 (0.03)	2.5 (0.2)
	2	19.7 (1)		10.42 (0.03)	
	3	43.9 (3)		10.13 (0.02)	

of the adsorbed protein. Part of the increase in electron density may arise from the presence of the DTT in the layers and the subphase.

As was the case for the urea-free system described above, 20 mM DTT in the presence of 6 M urea had little effect on the structure of the protein at the air−water interface. The solution containing DTT could be fitted with a three-layer model with layer thicknesses in agreement with those obtained from the protein in the DTT-free solution (data not shown).

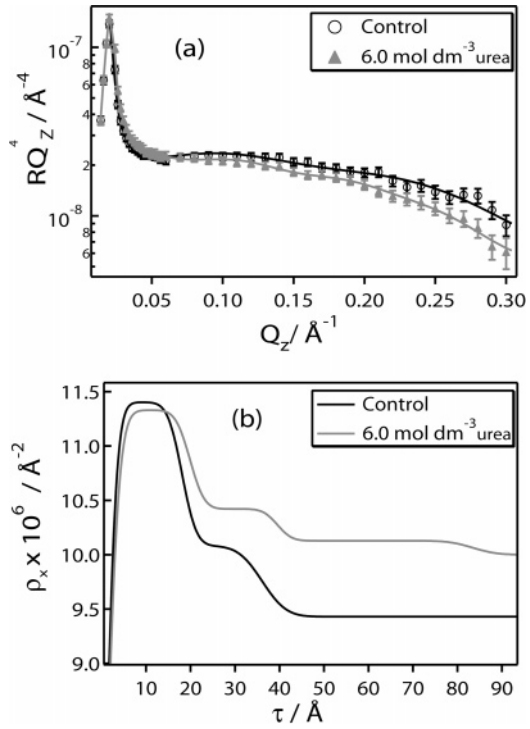

Figure 5. (a) RQ_z^4 vs Q_z X-ray reflectivities and fits (solid line) and (b) real-space X-ray scattering length density profiles obtained at the air−water interface from 10 mg mL^{-1}β-lactoglobulin solutions containing 0.0 (black) and 6.0 mol dm^{-3} (gray) urea.

When the DTT concentration was increased to 100 mM, there was a significant change in the surface structure, which is evident in Figure 8. The superimposed reflectivity profiles are vastly different fringe structures, as are the resulting X-ray scattering length density profiles. With 100 mM DTT present, the data could still be fitted using a three layer model, but with a 14 Å upper layer with a scattering length density lower than water. This surface structure is reminiscent of the guanidinium chloride denatured system where surface penetration, or dehydration, was discussed (section 3.2).

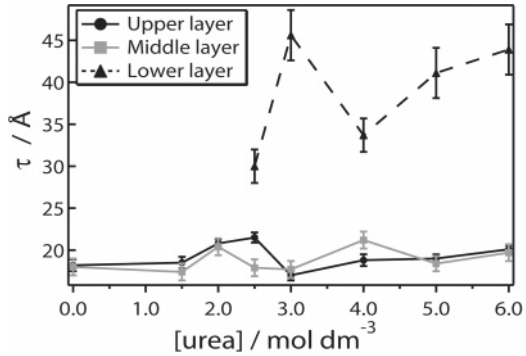

Figure 6. Variation of individual layer thicknesses with urea concentration. The upper layer (black circles and solid line) is adjacent to the air, and lower layer (black triangles and broken line) is adjacent the solution.

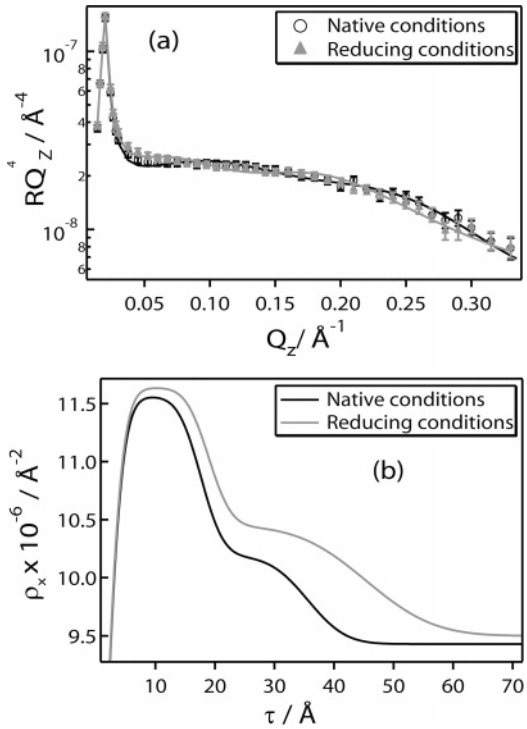

Figure 7. (a) RQ_z^4 vs Q_z X-ray reflectivities and fits (solid lines) and (b) real-space X-ray scattering length density profiles obtained at the air−water interface from 10 mg mL^{-1} β-lactoglobulin solutions under native (black line) and reducing conditions (gray line).

3.5. Effect of Chemical Denaturants on the Equilibrium Structure. For the β-lactoglobulin solutions containing G.HCl, reflectometry experiments were performed using both neutrons and X-rays. This allowed co-refinement of the data and subsequently the surface excesses to be computed without assumptions regarding a specific volume for the protein (2.2. Methodology, eq 4).

Figure 9a shows the dependence of the surface excess and the total layer thickness on the concentration of G.HCl. Introducing G.HCl to the system results in an immediate increase in the total thickness of the surface layer. In native solution conditions a total protein thickness of 38 Å is observed, which increases to 48 Å at [G.HCl] = 0.2 mol dm^{-3}. At 2.0 mol dm^{-3}, a plateau is reached with a total thickness of approximately 80 Å. During this expansion, there is little change in the surface excess. In fact, the surface excess remains constant at approximately 2 mg m^{-2} over the entire denaturant concentration range.

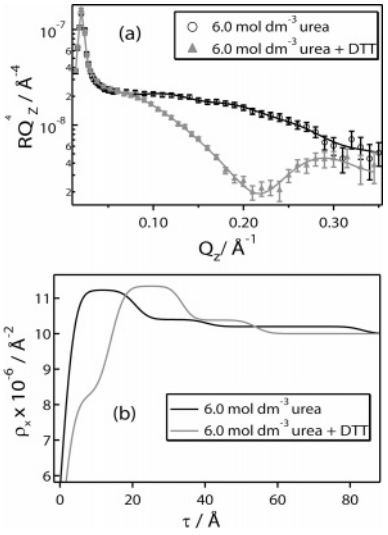

Figure 8. (a) RQ_z^4 vs Q_z X-ray reflectivities and fits (solid lines) and (b) real-space X-ray scattering length density profiles obtained at the air−water interface from 10 mg mL^{-1} β-lactoglobulin solutions containing 6.0 mol dm^{-3} urea in the presence of DTT (gray line) and in the absence of DTT (black line).

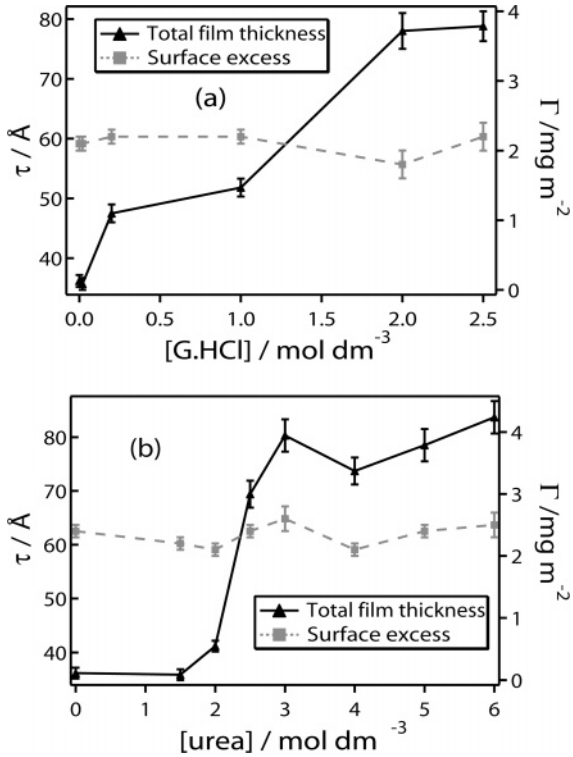

Figure 9. Variation of the surface excess (gray broken line) and the total layer thickness (black line) of β-lactoglobulin (black triangles) with (a) guanidinium chloride concentration and (b) urea.

Figure 9b shows the dependence of the surface excess and the total layer thickness on the concentration of urea. The surface parameters in this case were determined using X-ray reflectometry only. Thus, an estimated protein volume was necessary (2.2. Methodology, eq 7). Unlike the β-lactoglobulin solutions containing G.HCl, there is little change in the total thickness until [urea] = 2.0 mol dm^{-3}. At this concentration there was a small increase in the thickness as the layer expands from 38 to 41 Å. As the urea concentration was increased further, a rapid layer expansion occurred and a maximum total thickness of approximately 80 Å was reached at [urea] = 3.0 mol dm^{-3}. As

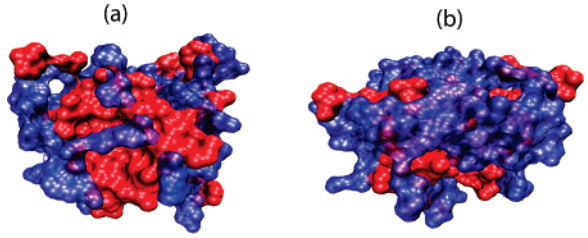

Figure 10. S.A.S.A. of the face of the monomer involved in dimerization (a) and the opposite face (b), showing the Hydrophobic regions (red) and hydrophilic regions (blue). Atomic coordinates for the structure were sourced from the Protein Data Bank (1B8E) and the molecular model was generated using visual molecular dynamics (VMD).[9,61,62]

was the case for the β-lactoglobulin solutions containing G.HCl, the surface excess remained constant over the entire denaturant range.

4. Discussion

4.1. Near-Native Conditions at the Air−Water Interface. The control experiments performed on protein solutions containing no chemical denaturant yielded a total layer thickness of approximately 36 Å for β-lactoglobulin (Table 1) in good agreement with previous layer thicknesses derived from neutron reflectometry measurements[14] of β-lactoglobulin at the air−water interface. The shortest axes of the β-lactoglobulin monomer and dimer are about 37 and 42 Å, respectively. From these dimensions, it is proposed that monomer adsorption is dominant, with little distortion of the globular framework upon adsorption. This proposal is supported by the work of Mackie et al., who reported preferential monomer adsorption by β-lactoglobulin at the air−water interface.[43]

The β-lactoglobulin dimer is stabilized by hydrogen bonds which form a surface loop and an antiparallel β-sheet,[9] and also by tight packing of hydrophobic residues at the interface between the monomers.[44] As a result, the dissociation constant (K_D) for β-lactoglobulin is quite small at only 5.4×10^{-4} (at pH 6.5 in phosphate buffer),[45] corresponding to a dimer fraction of 88% at a protein concentration of 10 mg mL^{-1}. Sakurai et al. calculated the change in the solvent accessible surface area (ΔS.A.S.A.) on dimer formation, showing a decrease in ΔS.A.S.A. of 1200 Å^2/dimer.[46] The larger proportion of this surface is hydrophobic, showing the hydrophobic effect to be a driving force for dimer formation. In Figure 10, the hydropathic distribution on the face of the monomer that forms the dimer interface is shown [Figure 10a], and for comparison the reverse side [Figure 10b] of the monomer is also displayed.

The longest axis of the dimer (76 Å) arises from the self-association of two monomers along their shortest axis (37 Å). Therefore, if the monomer adsorbs with the shortest axis perpendicular to the air−water interface, the face of the monomer that forms the dimer must be either: (a) in the direction of the solution bulk or (b) at the air−water interface. Based on the hydropathic distribution provided in Figure 10, scenario (b) is more likely and provides insight into why preferential monomer adsorption occurs. More specifically, the hydrophobic residues on the surface of the monomer that drive dimer formation are also responsible for the increased surface activity of the monomer, and conversely, if the monomers are arranged at the air−water interface with this hydrophobic surface near the air-phase, self-association is less favorable. Thus, the dissociation of this dimer by the interface to allow monomer adsorption illustrates the relative strengths of the protein−protein and the protein-surface interactions.

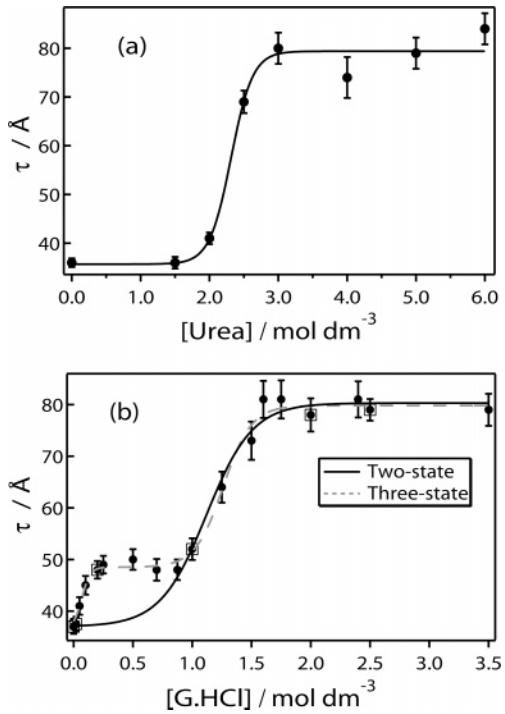

Figure 11. (a) Total film thickness of β-lactoglobulin as a function of urea concentration. Film thicknesses were derived from X-ray reflectometry datasets. The black line represents the best fit using eq 20. (b) Total film thickness of β-lactoglobulin as a function of guanidinium chloride concentration. Film thicknesses were derived from X-ray reflectometry datasets (black circle) and co-refined neutron and X-ray datasets (black circle with halo). The black line represents the best fit using eq 20 and the dashed gray line using eq 24.

TABLE 3: Thermodynamic Parameters of Urea-Induced Unfolding Transitions of β-Lactoglobulin at 25 °C

environment	pH	model	ΔG^0/ kJ mol^{-1}	m/ kJ mol^{-1} M^{-1}	$C_{1/2}$/ M
air−water interface	6.9	2 state	36 (8)	15 (3)	2.4
solution[47]	7	2 state	88 (3)	21.7 (0.8)	4.1

4.2. Chemical Denaturation Energetics. In order to compare the unfolding energetics of β-lactoglobulin at the air−water interface with the solution bulk, the total film thickness (τ) was used as an order parameter to define the equilibrium states in the denaturation pathway. For the present study, this appeared reasonable as the surface excess remained relatively constant for all concentrations of G.HCl and urea (Figure 9). Figure 11a displays the total film thickness of β-lactoglobulin as a function of urea concentration, where nonlinear regression was applied using eq 20 to yield the free energy of unfolding in the absence of a denaturant (ΔG^0), the rate of change of free energy as a function of denaturant concentration (m), and the urea concentration at which half of the protein molecules are denatured ($C_{1/2}$). These parameters are summarized in Table 3, and for comparison, thermodynamic parameters derived from urea denaturation of bovine β-lactoglobulin in solution[47] are also displayed.

The values of ΔG^0 and $C_{1/2}$ in Table 3 show that β-lactoglobulin is much less stable at the air−water interface than in solution at near-neutral pH. In both cases, a two-state model was used to extract the thermodynamic parameters which, for the air−water interface, describes the unfolding of native monomers into denatured monomers for reasons discussed above. In solution at pH 7, however, unfolding must also involve dissociation of the dimers, although a stable equilibrium

TABLE 4: Thermodynamic Parameters of G.HCl-Induced Unfolding Transitions of β-Lactoglobulin at 25 °C Using a 2 State Model

environment	pH	ΔG^0/ kJ mol^{-1}	m/ kJ mol^{-1} M^{-1}	$C_{1/2}$/ M
air−water	6.9	14.2 (1.4)	12.7 (1.5)	1.1
solution[50]	6	48.1 (2)	17.1 (2)	2.8

monomer state may not be evident if denaturation and dissociation are highly cooperative.

In a recent article, Hamada and Dobson used a three-state model to fit urea denaturation data after finding discrepancies between fluorescence intensities and peak positions in intrinsic tryptophan fluorescence spectra.[48] The three-state model involved a pre-denaturation dimer−monomer equilibrium with a value of $\Delta G^0_{DM} = 50.3$ (0.3) kJ mol^{-1}. This value is in excellent agreement with the difference between the solution and the surface free energies (52 kJ mol^{-1}) given in Table 3, supporting the structural evidence presented above for preferential monomer adsorption.

The correlation between the denaturant m value and the change in the solvent accessible surface area upon denaturation (ΔS.A.S.A.) was explored by Myers et al., who, after a study of a large set of proteins, developed the following empirical relationship for two-state urea denaturation[49]

$$\Delta\text{S.A.S.A.} = \frac{(m - 374)}{0.11} - 90s \qquad (4.1)$$

where s is the number of disulfide bonds and m is in units of cal mol^{-1} M^{-1}. The values of ΔS.A.S.A are about 30 000 (6000) Å^2 and 44 000 (1300) Å^2 for β-lactoglobulin at the air−water interface and in solution, respectively. The difference in these values is due in part to the decrease in ΔS.A.S.A upon dissociation (approximately 1200 Å^2 per dimer),[46] which would not occur for monomeric β-lactoglobulin adsorbed at the air−water interface. This contribution is only small, however, and it is likely that the structure of denatured β-lactoglobulin at the air−water interface is less unfolded than when in the bulk solution, a result of steric interactions at a crowded interface.

When G.HCl was used as the denaturant, an immediate change in the film thickness at low denaturant concentrations was observed, and plotting the total thickness as a function of denaturant concentration showed a curve shape that deviated from the single sigmoid observed for the urea-induced denaturation. To investigate this curve, a further 11 X-ray reflectometry experiments were performed and the data modeled to extract film thicknesses. Figure 11b displays the total film thickness of β-lactoglobulin as a function of G.HCl concentration. These thicknesses were modeled using nonlinear regression and a two-state model or a three-state model.

In most cases, chemical denaturation data from β-lactoglobulin at near neutral pH values is fitted using a two-state model, irrespective of whether G.HCl or urea is used as the denaturant.[27,45,47,50] In the example given above by Hamada and Dobson, the decision to use a three-state model was not based on obvious transitions in any given dataset but on deviations in the unfolding curves when a different observable property was used.[48] For these reasons, the data shown in Figure 11b was first fitted using a two-state equation describing native monomers in equilibrium with denatured monomers.

G.HCl is known to be a more powerful denaturant than urea,[42] which is reflected in the difference between the thermodynamic parameters summarized in Tables 3 and 4. By comparing the surface and solution bulk values of ΔG^0 and $C_{1/2}$, it is evident

TABLE 5: Thermodynamic Parameters of G.HCl-Induced Unfolding Transitions of β-Lactoglobulin at 25 °C Using a 3 State Model

environment	pH	ΔG^0_1/ kJ mol^{-1}	m_1/ kJ mol^{-1} M^{-1}	ΔG^0_2/ kJ mol^{-1}	m_2/ kJ mol^{-1} M^{-1}
air−water	6.9	8 (1.5)	68 (20)	26 (3)	20 (3)
solution[50]	2	38 (3)	12 (2)	16 (1)	4 (1)

that the structure of β-lactoglobulin is much less stable at the air−water interface, in line with the outcomes presented above for the urea denaturation experiments. That is, the difference between the solution and surface values of ΔG^0 arise from preferential monomer adsorption.

In Figure 11b, a three-state model (dotted line) has also been used to fit the denaturation data. This model describes denaturation of the β-lactoglobulin monomer via a monomeric intermediate. The accumulation of an equilibrium intermediate during G.HCl-induced unfolding of bovine β-lactoglobulin in solution has been reported but only at acidic pH values where the monomer is the dominant species;[50−52] summarized in Table 5 are the thermodynamic parameters resulting from fitting the data in Figure 11b to a three-state model. For comparison, the thermodynamic parameters reported by D'Alfonso et al. are also displayed.[50]

The three-state unfolding mechanisms differ greatly between the surface and the solution with respect to the stability of the intermediate state. At the surface, the intermediate state is reached almost immediately, resulting in a very low value of ΔG^0_1 (8 ± 1.5 kJ mol^{-1}) and a very large m value (68 kJ mol^{-1} M^{-1}). Conversely, in solution at pH 2, the native state is quite stable at $\Delta G^0_1 = 38 \pm 3$ kJ mol^{-1}. For the second transition (intermediate to the denatured state), the situation is reversed with the ΔG^0_2 at the surface being larger than ΔG^0_2 in solution.

Although the energetics of the pathways appear to differ greatly, the total free energy of unfolding in the absence of a denaturant ($\Delta G^0_{total} = \Delta G^0_1 + \Delta G^0_2$) is still significantly lower for the adsorbed protein, highlighting the contribution of the air−water interface to protein unfolding. In fact, good agreement is observed between the estimates of protein stability at the air−water interface using each denaturant, i.e., between ΔG^0_{total} for G.HCl (34 ± 3 kJ mol^{-1}) and ΔG^0 for urea (36 ± 8 kJ mol^{-1}).

Denaturant-dependent differences in the unfolding pathway of β-lactoglobulin are well documented and are likely related to the ionic nature of G.HCl. From the present study, there is no doubt that the structural response of the protein in the surface layer differed for each denaturant. The immediate increase in film thickness when using G.HCl may not simply be due to unfolding into the intermediate state. There may also be a change in orientation which would explain a subtle increase in the thickness, although at 47 Å the layer thickness is larger than any of the monomer dimensions.

Increasing the ionic strength has been shown to stabilize the β-lactoglobulin dimer for a number of salts including G.HCl when at acidic pH values.[46,53−55] For the present experiments, the solution pH was maintained near physiological pH (where the dimer is favored) and the concentration was high at 10 mg mL^{-1}. Thus, the observed increase in the film thicknesses at low G.HCl concentrations may have resulted from dimer adsorption, with the surface reflecting the behavior of the proteins in the solution bulk. A similar response was reported by Lu et al. for glucose oxidase adsorbed at the air−water interface,[56] although in this case monomer adsorption dominated at low ionic strengths and at high ionic strengths dimer adsorption occurred. It is unlikely that dimer adsorption would

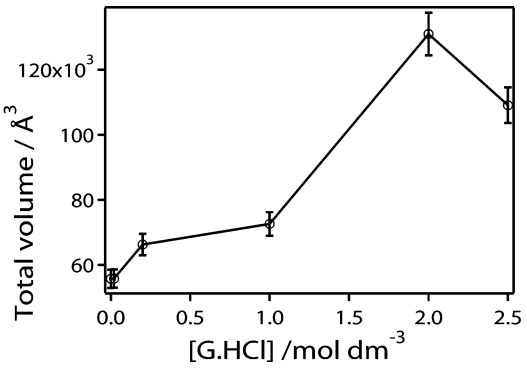

Figure 12. Average volume of a single β-lactoglobulin monomer as a function of G.HCl concentration. Volumes were calculated using eq 2.

result in a gradual increase in the film thickness representing the first transition; that is, dimer adsorption at the air−water interface would likely cause a sudden increase in the film thickness. However, dimer adsorption followed by a change in orientation resulting in an increase in film thickness cannot be ruled out. Note, however, that the total surface excess remains constant, implying dimer adsorption must be correlated with monomer desorption.

4.3. Denatured State. For β-lactoglobulin adsorbed at the air−water interface, denaturation, whether induced by urea or G.HCl, was evidenced by an increase in the film thickness from 36 to 80 Å. No increase in the surface excess was observed throughout the denaturation process, suggesting that a single discrete layer of protein was unfolding toward the subphase. At a protein concentration of 10 mg mL^{-1}, the surface layer is densely packed, which may promote unfolding in this direction.

Figure 12 displays the average volume occupied by a single β-lactoglobulin monomer at the air−water interface as a function of G.HCl concentration. When no denaturant was present, the volume occupied by a single β-lactoglobulin monomer at the air−water interface was 55×10^3 Å.[3] The volume per monomer, estimated using unit cell dimensions, is 38×10^3 Å.[3,12] The reasonable agreement between these volumes shows the ability of β-lactoglobulin to form a single densely packed layer of protein molecules at the air−water interface. At [G.HCl] > 2 mol dm^{-3}, a greater than 2-fold increase in the average volume was observed, signifying expansion of the globular structure in the direction of the solution upon denaturation. A 2-fold increase in the volume of β-lactoglobulin after G.HCl-induced denaturation was also reported by D'Alfonso et al., who suggested that, though somewhat expanded, the denatured protein still retains a fairly compact conformation.[27]

The structure of the β-lactoglobulin adsorbed at the water interface in the denatured state was dependent on the denaturant used, even though the interfacial layer thicknesses were similar. For urea-denatured β-lactoglobulin at [urea] = 6 mol dm^{-3}, the surface protein layer contained three regions of decreasing protein density in the direction of the subphase (Figure 5). When G.HCl was used at 3.5 mol dm^{-3}, 14 Å of the protein was exposed to the air phase. We suggest that the hydrophobic regions, now free of the globular constraints, may be in part surface exposed. For this to be true, the structure of the surface molecule at 3.5 mol dm^{-3} G.HCl would have to differ from the urea-denatured molecule. This scenario is supported by the similarity in the urea-denatured structure when 100 mM DTT was present, i.e., disulfide bond reduction resulting in greater flexibility in the protein structure (Figure 8). Another factor which may contribute to surface exposure is the change in the solution conditions arising from the increase in ionic strength upon the addition of G.HCl. It is well-known that the presence of chaotropic salts such as G.HCl affect the forces between proteins, as accessed by measurements of the second virial coefficient.[57−59]

At 20 mM, the reducing agent DTT appeared to have little effect on the structure of β-lactoglobulin adsorbed at the air−water interface whether urea was present or not. This was not the case when the concentration was increased to 100 mM, suggesting incomplete or no reduction on the disulfide bonds at the lower concentration. When free of urea, the thickness increase in the lower layer when DTT was present shows a more extended structure, indicating distortion of the globular fold. Min et al. showed that the presence of disulfide bonds stabilized the structure of lysozyme adsorbed at the air−water interface.[21] In contrast, the solution structure of lysozyme has been shown to maintain a globular structure when free of disulfide bonds,[60] which suggests surface-induced distortion of the globular fold for reduced proteins adsorbed at the air−water interface.

5. Conclusion

From the present study, it has been shown that β-lactoglobulin retains its globular structure when adsorbed at the air−water interface, with a film thickness close to the shortest axis of the monomer. Adsorption destabilizes the tertiary structure resulting in chemical denaturation at lower denaturant concentrations than necessary for denaturation in solution. The difference in the free energies of chemical denaturation between solution and surface is found to correspond well with the free energy of dimerization of the protein. This implies that the destabilizing effect is due to the fact that the monomer, which is less stable to chemical denaturant, is found to be preferentially adsorbed at the surface, β-lactoglobulin in bulk solution at pH 6.85 predominantly exists as dimers.

For β-lactoglobulin adsorbed at the air−water interface at pH 6.85, the unfolding pathway was described using a two-state model for urea, involving the equilibrium between native monomers and denatured monomers. When G.HCl was used as the denaturant, a three-state model involving an equilibrium intermediate was appropriate.

Acknowledgment. AINSE (Australian Instituite of Nuclear Science and Engineering) for funding through the AINSE Post-Graduate Research Award. Travel to the RAL was funded through the Access to Major Research Facilities Program administered by ANSTO (Australian Nuclear Science and Technology Organization).

References and Notes

(1) Furie, B.; Furie, B. C. *J. Clin. Invest.* **2005**, *115*, 3355.
(2) Dickinson, E. *An Introduction to Food Colloids*; Oxford University Press: Oxford, 1992.
(3) Dexter, A. F.; Malcolm, A. S.; Middelberg, A. P. J. *Nat. Mater.* **2006**, *5*, 502.
(4) Rusmini, F.; Zhong, Z. Y.; Feijen, J. *Biomacromolecules* **2007**, *8*, 1775.
(5) Pace, C. N.; Shaw, K. L. *Proteins: Struct., Funct., Genet.* **2000**, *41*, 1.
(6) Crowfoot, D. M.; Riley, D. P. *Nature* **1938**, *141*, 521.
(7) Jenness, R. In *Milk Proteins Chemistry and Molecular Biology*; McKenzie, H. A., Ed.; Academic Press: New York, 1970; Vol. 1.
(8) Papiz, M. Z.; Sawyer, L.; Eliopoulos, E. E.; North, A. C. T.; Findley, J. B. C.; Sivaprasadarao, R.; Jones, T. A.; Newcomer, M. E.; Kraulis, P. J. *Nature* **1986**, *324*, 383.
(9) Brownlow, S.; Cabral, J. H. M.; Cooper, R.; Flower, D. R.; Yewdall, S. J.; Polikarpov, I.; North, A. C. T.; Sawyer, L. *Structure* **1997**, *5*, 481.
(10) Qin, B. Y.; Bewley, M. C.; Creamer, L. K.; Baker, H. M.; Baker, E. N.; Jameson, G. B. *Biochemistry* **1998**, *37*, 14014.

(11) Kawata, K.; Hoshino, M.; Forge, V.; Era, S.; Batt, C. A.; Goto, Y. *Protein Sci.* **1999**, *8*, 2541.
(12) Oliveira, K. M. G.; Valente-Mesquita, V. L.; Botelho, M. M.; Sawyer, L.; Ferreira, S. T.; Polikarpov, I. *Eur. J. Biochem.* **2001**, *268*, 477.
(13) Adams, J. J.; Anderson, B. F.; Norris, G. E.; Creamer, L. K.; Jameson, G. B. *J. Struct. Biol.* **2005**, *154*, 246.
(14) Atkinson, P. J.; Dickinson, E.; Horne, D. S.; Richardson, R. M. *J. Chem. Soc., Faraday Trans.* **1995**, *91*, 2847.
(15) Marsh, R. J.; Jones, R. A. L.; Sferrazza, M.; Penfold, J. *J. Colloid Interface Sci.* **1999**, *218*, 347.
(16) Meinders, M. B. J.; De Jongh, H. H. J. *Biopolymers* **2002**, *67*, 319.
(17) Martin, A. H.; Meinders, M. B. J.; Bos, M. A.; Cohen Stuart, M. A.; van Vliet, T. *Langmuir* **2003**, *19*, 2922.
(18) Graham, D. E.; Phillips, M. C. *J. Colloid Interface Sci.* **1979**, *70*, 403.
(19) Birdi, K. s. *J. Colloid Interface Sci.* **1973**, *43*, 545.
(20) Tanford, C. *J. Amer. Chem. Soc.* **1962**, *84*, 4240.
(21) Min, D. J.; Winterton, L.; Andrade, J. D. *J. Colloid Interface Sci.* **1998**, *197*, 43.
(22) Shortle, D. *Nat. Struct. Biol.* **1999**, *6*, 203.
(23) Breslow, R.; Guo, T. *P. Natl. Acad. Sci. U.S.A.* **1990**, *87*, 167.
(24) Batchelor, J. D.; Olteanu, A.; Tripathy, A.; Pielak, G. J. *J. Am. Chem. Soc.* **2004**, *126*, 1958.
(25) Dohnal, V.; Costas, M.; Carrillo-Nava, E.; Hovorka, S. *Biophys. Chem.* **2001**, *90*, 183.
(26) Schellman, J. A. *Biophys. Chem.* **2002**, *96*, 91.
(27) D'Alfonso, L.; Collini, M.; Baldini, G. *Biochemistry* **2002**, *41*, 326.
(28) Dempsey, C. E.; Piggot, T. J.; Mason, P. E. *Biochemistry* **2005**, *44*, 775.
(29) Mason, P. E.; Neilson, G. W.; Enderby, J. E.; Saboungi, M. L.; Dempsey, C. E.; MacKerell, A. D.; Brady, J. W. *J. Am. Chem. Soc.* **2004**, *126*, 11462.
(30) http://www.isis.rl.ac.uk
(31) Brown, A. S.; Holt, S. A.; Saville, P. M.; White, J. W. *Aust. J. Phys.* **1997**, *50*, 391.
(32) Henderson, M. J.; Perriman, A. W.; Robson-Marsden, H.; White, J. W. *J. Phys. Chem. B* **2005**, *109*, 20878.
(33) Penfold, J. In *Neutron, X-ray and Light Scattering*; Lindner, P., Zemb, T., Eds.; North-Holland: Amsterdam, 1991; pp 223.
(34) Kawahara, K.; Tanford, C. *J. Biol. Chem.* **1966**, *241*, 3228.
(35) Mande, S. C.; Sobhia, M. E. *Protein Eng.* **2000**, *13*, 133.
(36) Courtenay, E. S.; Capp, M. W.; Record, M. T. *Protein Sci.* **2001**, *10*, 2485.
(37) Macaskill, J. B.; Robinson, R. A.; Bates, R. G. *J. Chem. Eng. Data* **1977**, *22*, 411.
(38) Cavallo, L.; Kleinjung, J.; Fraternali, F. *Nucleic Acids Res.* **2003**, *31*, 3364.
(39) Holt, S. A.; McGillivray, D. J.; Poon, S.; White, J. W. *J. Phys. Chem. B* **2000**, *104*, 7431.
(40) Lu, J. R.; Su, T. J.; Thomas, R. K.; Penfold, J.; Webster, J. *J. Chem. Soc., Faraday Trans.* **1998**, *94*, 3279.
(41) Jacrot, B. *Rep. Prog. Phys.* **1976**, *39*, 911.
(42) Greene, R. F., Jr.; Pace, C. N. *J. Biol. Chem.* **1974**, *249*, 5388.
(43) Mackie, A. R.; Husband, F. A.; Holt, C.; Wilde, P. J. *Int. J. Food Sci. Technol.* **1999**, *34*, 509.
(44) Qin, B. Y.; Bewley, M. C.; Creamer, L. K.; Baker, E. N.; Jameson, G. B. *Protein Sci.* **1999**, *8*, 75.
(45) Sakai, K.; Sakurai, K.; Sakai, M.; Hoshino, M.; Goto, Y. *Protein Sci.* **2000**, *9*, 1719.
(46) Sakurai, K.; Oobatake, M.; Goto, Y. *Protein Sci.* **2001**, *10*, 2325.
(47) Yagi, M.; Sakurai, K.; Kalidas, C.; Batt, C. A.; Goto, Y. *J. Biol. Chem.* **2003**, *278*, 47009.
(48) Hamada, D.; Dobson, C. M. *Protein Sci.* **2002**, *11*, 2417.
(49) Myers, J. K.; Pace, C. N.; Scholtz, J. M. *Protein Sci.* **1995**, *4*, 2138.
(50) D'Alfonso, L.; Collini, M.; Ragona, L.; Ugolini, R.; Baldini, G.; Molinari, H. *Proteins: Struct., Funct., Bioinf.* **2005**, *58*, 70.
(51) Ananthanarayanan, V. S.; Ahmad, F.; Bigelow, C. C. *Biochim. Biophys. Acta* **1977**, *492*, 194.
(52) Hamada, D.; Goto, Y. *J. Mol. Biol.* **1997**, *269*, 479.
(53) Townend, R.; Winterbottom, R. J.; Timasheff, S. N. *J. Am. Chem. Soc.* **1960**, *82*, 3161.
(54) Joss, L. A.; Ralston, G. B. *Anal. Biochem.* **1996**, *236*, 20.
(55) Baldini, G.; Beretta, S.; Chirico, G.; Franz, H.; Maccioni, E.; Mariani, P.; Spinozzi, F. *Macromolecules* **1999**, *32*, 6128.
(56) Lu, J. R.; Su, T. J.; Georganopoulou, D.; Williams, D. E. *J. Phys. Chem. B* **2003**, *107*, 3954.
(57) Ho, J. G. S.; Middelberg, A. P. J.; Ramage, P.; Kocher, H. P. *Protein Sci.* **2003**, *12*, 708.
(58) Bostrom, M.; Williams, D. R. M.; Ninham, B. W. *Curr. Opin. Colloid Interface Sci.* **2004**, *9*, 48.
(59) Bostrom, M.; Tavares, F. W.; Finet, S.; Skouri-Panet, F.; Tardieu, A.; Ninham, B. W. *Biophys. Chem.* **2005**, *117*, 217.
(60) Chang, J. Y.; Li, L. *FEBS Lett.* **2002**, *511*, 73.
(61) Deshpande, N.; Addess, K. J.; Bluhm, W. F.; Merino-Ott, J. C.; Townsend-Merino, W.; Zhang, Q.; Knezevich, C.; Xie, L.; Chen, L.; Feng, Z. K.; Green, R. K.; Flippen-Anderson, J. L.; Westbrook, J.; Berman, H. M.; Bourne, P. E. *Nucleic Acids Res.* **2005**, *33*, D233.
(62) Humphrey, W.; Dalke, A.; Schulten, K. *J. Mol. Graphics* **1996**, *14*, 33.